ELSEVIER

Catalysis Today 32 (1996) 63–70

CATALYSIS TODAY

Epoxidation of olefines with PDMS membranes containing zeolite occluded manganese diimine complexes

P.P. Knops-Gerrits, I.F.J. Vankelecom, E. Béatse, P.A. Jacobs

Centrum voor Oppervlaktechemie en Katalyse, Katholieke Universiteit Leuven, Kardinaal Mercierlaan 92, B-3001 Heverlee, Belgium

Abstract

A new composite catalyst for selective epoxidation of olefins with *tert*-butyl hydroperoxide (*t*BHP) is reported. The catalyst contains manganese diimine complexes (*cis*-Mn bis-*2,2'*-Bipyridyl), occluded within a NaY zeolite, in turn incorporated in a polydimethylsiloxane membrane (*cis*-$[Mn(bpy)_2]^{2+}$-NaY-PDMS). The three-step synthesis consists of a Mn^{2+} exchange of NaY, ligand sorption to form *cis*-$[Mn(bpy)_2]^{2+}$-NaY and incorporation of the latter in a PDMS membrane. The major differences between $[Mn(bpy)_2]^{2+}$-NaY as such and occluded in PDMS are observed in the sorption and catalytic characteristics. With the membrane system, the use of a solvent becomes obsolete. Whereas optimal cyclohexene oxidation with $[Mn(bpy)_2]^{2+}$-NaY occurs with hydrogen peroxide in acetone, tBuOOH proves to be a better oxidant for $[Mn(bpy)_2]^{2+}$-NaY-PDMS. The reactions in batch and fed-batch reactors are discussed. A simple regeneration procedure, monitored by FT-IR spectroscopy is proposed.

Keywords: Oxidation catalysis; Manganese complex; PDMS; Zeolites; Peroxides; Cyclohexene; Styrene

1. Introduction

Manganese is active in mononuclear metallo-enzymes [1,2] involved in redox processes in the metabolism of oxygen such as superoxide dismutase (SOD) or pyruvate carboxylase. As Mn (bi)pyridyl complexes [2–5] mimic the active sites of such enzymes, the zeolite encaged complexes, embedded in turn a PDMS membrane are inorganic mimics of enzymes. The zeolites play the proteic role and the hydrofobic membranes mimic the biological membrane embedding the enzyme. With iron phthalocyanine-NaY-PDMS systems a formal as well as mechanistic mimicry of Cytochrome P-450 is achieved [6]. In NaY, Mn, VO and Ru bis-bipyridine complexes [7–14] have been occluded as well. Parallel research has focused on pendant polymer tris Ru complexes [15,16]. Olefin epoxidation has been reported with homogeneous Mn tetra-phenyl-porphyrin (TPP), Mn Schiff-base, Fe or Ru poly-pyridines [17–20] and with the heterogeneous $[Mn(bpy)_2]^{2+}$-NaY and $[VO(bpy)_2]^{2+}$-NaY catalysts [10–12]. In the present work, the latter catalyst was embedded in a PDMS membrane and its catalytic behaviour in epoxidation reactions examined. The role of solvents was studied as well as the membrane regeneration procedure.

2. Experimental

Manganese(II)acetate, 2,2'-bipyridine, hydrogen peroxide (35% in water), acetone, aceto-

PII S0920-5861(96)00179-4

nitrile, dichloromethane, methanol, ethanol, cyclohexene, styrene (all +99%) were purchased from ACROS Chimica. A sample of NaY from Zeocat, with Si/Al ratio of 2.46 was used. PDMS (RTV615) was purchased from General Electric, New York.

The Mn_8-NaY zeolite (8 Mn ions per unit cell, corresponding to one ion per supercage) was obtained by the exchange of Na for Mn for 3 h in a 2 mM solution of $Mn(CH_3COO)_2$ adjusted to pH 5.5 with HCl. As such the Mn^{2+} is present in a Na^+ acetate/acetic acid buffer to avoid its precipitation. The Mn_8-NaY zeolite was washed, filtered and then dried overnight in an open petri-dish at 293 K followed by drying it under a continuous flow of 100 ml/min of N_2. The temperature was raised from 293 K to 423 K at a rate of 1 K/min and maintained at 423 K for 15 h. After drying the zeolite contains about 32.8 water molecules per unit cell. In an inert atmosphere ligand was added to MnNaY in a 2.5:1 ligand: Mn molar ratio. The dry mixture was heated at a rate of 1 K/min under a continuous flow of 100 ml/min of N_2 and maintained at 363 K in a closed cell for at least two days. The zeolite was soxhlet-extracted with CH_2Cl_2 for 24 h in order to allow extraction of the unreacted ligand. Thermogravimetric and elementary analysis showed the presence of one $[Mn(bpy)_2]^{2+}$ complex per supercage.

PDMS-membranes are prepared as described by Vankelecom et al. [6]. The crosslinking agent (RTV 615B) and the prepolymer (RTV 615A) are mixed and cast on a glass plate. The plate is heated for 30 min at 423 K under vacuum, during which the crosslinking agent and the prepolymer chains form a strong elastic membrane. Zeolite (42 wt%), prepolymer and crosslinking agent are mixed in three consecutive steps. (1) The zeolite powder is sieved (mesh size = 0.16 mm) and consequently dried for one hour under vacuum at 573 K. 6.5 g dried zeolite is dispersed in 40 g methylisobutylketone by placing the solution in an ultrasonic bath for 1 h. (2) 1.4 g of crosslinking agent is added to the solution and the resulting mixture is stirred for 2 h. (3) 14 g of prepolymer is added to the mixture and this is stirred again for 1 h, respecting a 1:10 crosslinking agent/prepolymer ratio. The mixture is placed under vacuum for 5 min to remove entrapped air, before casting the membrane on the glass plate. The mixture is homogeneously spread as a layer with a thickness of 0.25 mm. The glass plate is heated for 1 h in an oven at 573 K under vacuum. *FT-IR spectra* were recorded on a NICOLET-730 FT-IR instrument. DRS spectra were recorded on a VARIAN Cary 5 spectrophotometer. *Molecular modelling* was done with the program Hyperchem 3.0 for Windows (HYPERCUBE, Inc.). *Catalytic reactions* were performed in a 10 ml Parr reactor, a 10ml glass batch reactor, a 100 ml glass perfusor reactor system in which 6 cm^2 of membrane is mounted. For a 10 ml reaction vessel 0.02 mmol catalyst, 25–40 mmol substrate and 5 ml of solvent are mixed. For 100 ml reaction vessel 0.1 mmol catalyst, 200–300 mmol substrate and 35 ml of solvent are mixed. H_2O_2 or TBHP is added with a perfusor at a rate of 20 mmol/h for 10–15 h. After the reaction, peroxide efficiencies were determined using cerimetric titrations. Product analysis was done with GC on a 50 m CP Sil-WAX-52 CB capillary column from Chrompack and with GC-MS.

3. Results and discussion

3.1. Spectroscopy

FT-IR on the *cis*-$[Mn(bpy)_2]^{2+}$-NaY-PDMS system shows the combination of complex, zeolite and PDMS absorption bands. The occluded complex shows no major frequency changes from the homogeneous *cis*-$[Mn(bpy)_2]^{2+}$ complex [21]. The synthesised $[Mn(bpy)_2]^{2+}$-NaY contains a majority of *cis* complexes. The spectra of homogeneous *cis*- and *trans*-bipyridyl only show a difference in the bands at *757 cm^{-1} (m) and 772 cm^{-1} (s)*. This difference can be explained in terms of symmetry of these

complexes: the highly symmetrical $[Mn(bpy)_3]^{2+}$ (D_3) and *trans*-$[Mn(bpy)_2]^{2+}$ (D_{2h}) have a single band for the C–H out-of-plane deformation. When the symmetry is lowered as in *cis*-$[Mn(bpy)_2]^{2+}$ (C_2), the splitting of this strong band in two bands of medium intensity occurs. The 758 cm^{-1} C–H out-of-plane deformation absorption band of bpy [22,23] in the Na bpy-Y spectrum shifts 10 cm^{-1} upon complexation to 768 cm^{-1}. For the $[Mn(bpy)_2]^{2+}$-NaY complexes, the broad maximum occurs at 772 cm^{-1} with a shoulder at 767 cm^{-1}, indicative for a major fraction of cis-coordinated complex. For PDMS important asymmetric deformation bands of CH_3 in $SiCH_3$ are seen at 1413 and 1445 cm^{-1}. In *Diffuse Reflectance spectra*, the pink colour of the zeolite and its derived PDMS membrane indicates the presence of a Mn^{II} to bipyridine Metal to Ligand (bpy) Charge Transfer (MLCT) at 530 nm [10,11]. *Molecular modelling* shows no zeolite supercage (1.3 nm diameter) distortion after inclusion of a $[Mn(bpy)_2]^{2+}$ complex (1.2 nm diameter). The structure of the composite membrane catalyst system is shown in Fig. 1.

3.2. Epoxidation catalysis with tert-butyl hydroperoxide

In catalytic epoxidation, optimal diffusion of oxidant and substrate to the active site as well as transport of products back to the bulk solution, are key concerns. Cyclohexene and styrene are epoxidised with the oxidantia H_2O_2 and *t*BHP in presence and absence of solvents. The ratio Mn-sites/mmol substrate/mmol oxidant

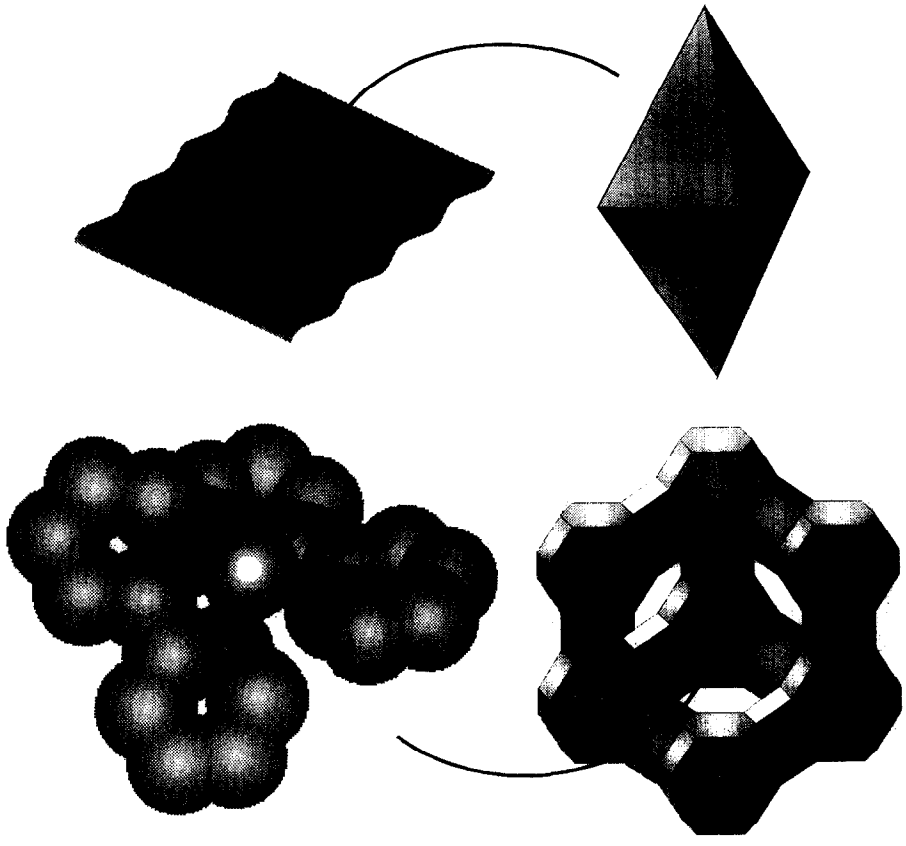

Fig. 1. The structural architecture of *cis*-$[Mn(bpy)_2]^{2+}$-NaY-PDMS. A dimensional trip. Bottom left: Mn, N and C atoms of *cis*-$[Mn(bpy)_2]^{2+}$, bottom right: the NaY supercage, top right: the cubic faujasite NaY crystal and top left: the PDMS membrane.

is varied according to the reactor-type. From sorption measurements of reactants and possible solvents in the composite catalyst, it is clear that the reaction medium imposes large differences on membrane swelling (Fig. 2). Catalytic activity is affected by solvents, since they sorb competitively with the substrate at the active site. $[Mn(bpy)_2]^{2+}$-NaY-PDMS is optimally used in fed-batch reactors, with low oxidant concentrations, since batch reaction with higher concentrations lead to more oxidant decomposition by free Mn^{2+} and efficiency decrease, resulting in lower activity.

The *cyclohexene epoxidation* activity in time is shown in Fig. 3. In absence of solvent, a high activity is seen in the reaction: a T.O.N. (Turn-Over-Number) of 100 is reached after 10 h, at an initial T.O.F. (Turn-Over-Frequency) of 15–10 h^{-1}. In acetone, the epoxidation is much slower and the lower apparent T.O.F. around 0.5 h^{-1} remains fairly constant over time. In octane, results are in between both extremes with a T.O.N. around 32 after 10 h and T.O.F. around 3 h^{-1}, again due to competitive sorption at the active sites, therefor reducing the apparent T.O.F. In all these cases for the first 125 h only substrate depletion occurs and no catalyst

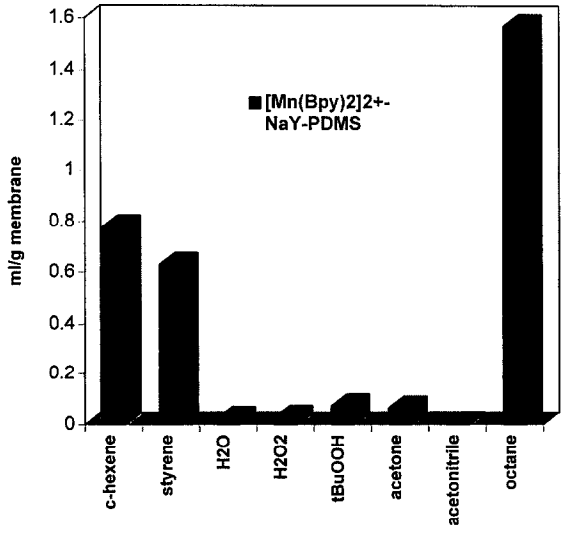

Fig. 2. Sorption of pure solvent, substrate and oxidantia at 25°C on c*is*-$[Mn(bpy)_2]^{2+}$-NaY-PDMS.

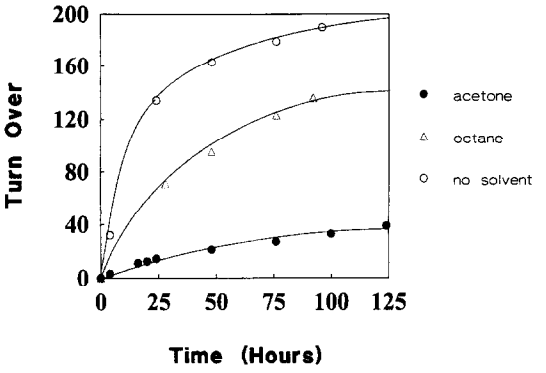

Fig. 3. Oxidation of cyclohexene with c*is*-$[Mn(bpy)_2]^{2+}$-NaY-PDMS and *t*BHP in time. Ratio Mn/cyclohexene/*t*BHP: 1/300/2100 in acetone and octane, 1/2500/2500 in absence of solvent.

deactivation in time is seen. These results can be rationalised in terms of the polarity of the different phases and reagents. In order to allow diffusion of the reagents through the polymer network towards the zeolite, the PDMS should be swollen. As shown in Fig. 2, this is especially the case for octane and cyclohexene, but not at all for acetone. Additionally, the solvent can sorb competitively with the reagents in the zeolite. Acetone, being far more polar than octane and cyclohexene, shows a stronger affinity for the zeolite. The activity for the epoxidation of cyclohexene with *t*BHP (Fig. 3) increases in the following solvent order: acetone < octane < cyclohexene. In absence of solvent the highest activity is obtained. Indeed, in cyclohexene and octane the PDMS is strongly swollen, enabling fast diffusion of reagents. Octane, despite of being apolar, will still be sorbed in the zeolite and compete with the reagents for sorption near the active sites. In absence of solvent, every site will be available for epoxidation. Competitive sorption on the zeolite of products, that are more polar than the substrate (e.g., 1,2-cyclohexanediol or others), block the accessibility of new substrate molecules to the zeolite cage, explaining the gradual decrease of the reaction rate in time.

The Mn is thought to be stabilised in a high-valent $(bpy)_2Mn^{IV}O$ state, and this is the

active site for epoxidation. The product distribution for the batch and fed-batch reactors is given in Table 1. In absence of solvent, the amount of allylic products formed is negligable compared to cyclohexene oxide, 1,2-cyclohexanediol and 2-*tert*-butoxy-cyclohexanol. For oxidations with *t*BHP in acetone more cyclohexen-3-one is formed via allylic oxidation. As in the kinetics of homogeneous catalytic epoxide opening, protonation and not nucleophilic attack determines the rate. Thus, bifunctional characteristics originate from the presence of acid sites stemming from Mn^{2+} hydrolysis and cation deficiencies next to the epoxidation sites. *Tert*-butanol formed from *t*BHP easily desorbs from the zeolite (it sorbs well in the membrane), limiting the 2-*tert*-butoxy-cyclohexanol formation, yielding mainly 1,2-cyclohexanediol. In absence of acetone, more *tert*-butanol stays in the zeolite and more 2-*tert*-butoxy-cyclohexanol is formed.

The *styrene epoxidation* in time is shown in Fig. 4. The initial strong activity of the catalytic system for the first 30 h is independent of the use of a solvent with a T.O.N. (Turn-Over-Number) of 90 after 30 h, and initial T.O.F. (Turn-Over-Frequency) of 3 h^{-1}. The catalyst keeps its initial activity in absence of solvent for 125 h and still has a T.O.F. of 3 h^{-1}. The activity is lower in acetone compared to octane.

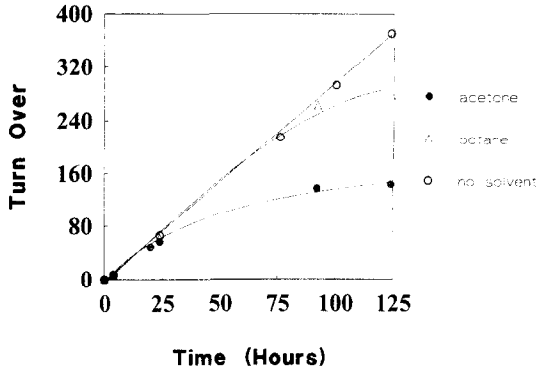

Fig. 4. Oxidation of styrene with *cis*-$[Mn(bpy)_2]^{2+}$-NaY-PDMS and *t*BHP in time. Ratio Mn/ cyclohexene/*t*BHP: 1/500/3500 in acetone and octane, 1/2500/2500 in absence of solvent.

Styrene is more polar than cyclohexene and sorbs slightly less in the membrane. Due to its activated double bond it is more reactive. Being more polar, it competes stronger with acetone in the zeolite sorption. The product distribution is shown in Table 2. Epoxidation gives the styrene-oxide (1), its reactive oxirane ring can be hydrated on Brönsted acid sites to give 1,2-dihydroxy-1'-phenyl-ethane (2), or undergo further oxidation with C–C bond splitting to benzaldehyde (3) and formaldehyde (4). In the styrene epoxidation, selectivity changes by the solvent are of minor importance (Table 2). Ox-

Table 1
Cyclohexene epoxidation with cis-$[Mn(bpy)_2]^{2+}$-NaY-PDMS

Reactor	Oxidant	Solvent	TON	Selectivity (%)				
				Cyclohexene-oxide	Cyclohexane-diol	2-t-butoxy-cyclohexanol, * ketal	Cyclohexanol	Cyclohexenone
Batch	H_2O_2 [a]		15		100			
Batch	*t*BHP [b]		11	40	40	12	6	2
Batch	*t*BHP [c]		22	20	30	42	3	5
Fed-batch	*t*BHP [d]		196	4	37	55	4	
Fed-batch	*t*BHP [e]	acetone	36	9	54	14 *	6	16
Fed-batch	*t*BHP [f]	octane	137	11	65	21	3	

Reaction conditions: a–c in a Parr microreactor and d–f in a Perfusor reactor.
[a] 0.02 mmol cat; 40 mmol chexene; 200 mmol H_2O_2, 100 h.
[b+c] 0.02 mmol cat; 20 mmol chexene; 80 mmol *t*BHP, 20 h, 70 h.
[d] 0.1 mmol cat; 250 mmol chexene; 250 mmol *t*BHP; 125 h.
[e+f] 0.1 mmol cat; 30 mmol chexene, 30 ml solvent, 210 mmol *t*BHP; 125 h.

Table 2
Styrene epoxidation with cis-$[Mn(bpy)_2]^{2+}$-NaY-PDMS

Reactor	Oxidant	Solvent	TON	Selectivity		
				Oxide	Benzal-dehyde	Ketal
Batch	H_2O_2 [a]		42	0	100	
Batch	*t*BHP [b]	Octane	3	72	28	
Batch	*t*BHP [c]	Octane	13	45	55	
Fed-batch	*t*BHP [d]		48	80	20	
Fed-batch	*t*BHP [e]		402	19	81	
Fed-batch	*t*BHP [f]	Acetone	121	11	74	15
Fed-batch	*t*BHP [g]	Octane	264	45	55	

Reaction conditions: a–c in Parr microreactor and d–f in a perfusor reactor.
[a] 0.02 mmol cat; 40 mmol styrene; 200 mmol H_2O_2, 20 h;
[b+c] 0.02 mmol cat; 2.25 mmol styrene; 100 mmol octane; 6.75 mmol *t*BHP, 4 h; 70 h;
[d+e] 0.1 mmol cat; 250 mmol styrene, 250 mmol *t*BHP; 12.5 h; 125 h;
[f+g] 0.1 mmol cat; 50 mmol styrene, 30 ml solvent, 350 mmol *t*BHP; 125 h.

idative C–C bond splitting is typical for Mn oxidation. Epoxide, benzaldehyde and formaldehyde are seen in the absence of acetone. In acetone oxidation, catalytic acidification of the reaction medium can lead to (2) and ketal (5) formation. Consequently, pronounced bifunctionality favors further oxidation.

3.3. Influence of the oxidantia and their ratio.

With H_2O_2, reaction in batch reactors is only seen if oxidant decomposition with O_2 formation by Mn is impeded in sealed Parr microreactors. In fed-batch reactions with low H_2O_2 concentrations, again the very low active site accessibility is caused by the low amount of H_2O_2 sorption in the hydrofobic membrane (Fig. 2). This in turn affects the peroxide efficiency for H_2O_2 reactions negatively (Fig. 5). The absence of activity contrasts with the good epoxidation results with H_2O_2 and $(Mn(bpy)_2)^{2+}$-NaY in absence of PDMS. The water formed, prefers the zeolite over the PDMS membrane due to its polarity, and hinders further diffusional uptake of substrate and reaction. Epoxidation with the well sorbing *t*BHP leads to formation of *t*butanol. *t*Butanol is a voluminous alcohol significantly less polar than water, that sorbs better in PDMS than *t*BHP. It thus desorbs easily from the zeolite, allowing further substrate and oxidant sorption.

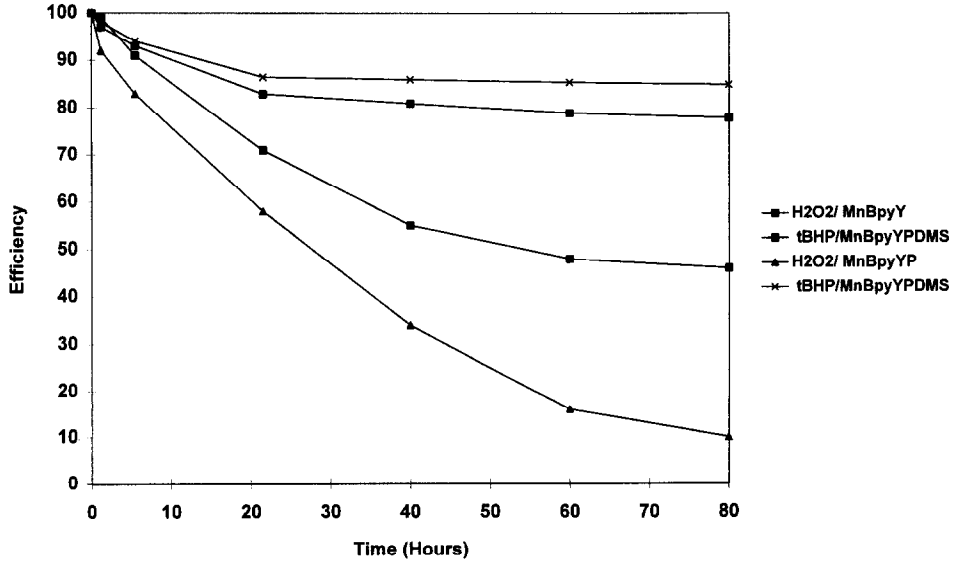

Fig. 5. Comparison of the peroxide efficiency in *t*BHP (determined by GC) and H_2O_2 (determined by GC and cerimetric analysis) in the cyclohexene epoxidation with c*is*-$[Mn(bpy)_2]^{2+}$-NaY-PDMS in a fed-batch reaction.

Comparing Tables 1 and 2, styrene shows higher activity than cyclohexene. The peroxide efficiency for *t*BHP and H_2O_2 in the epoxidation of cyclohexene is shown in Fig. 5. Whereas for *t*BHP the peroxide efficiency increases from 78% to 85% in PDMS, it decreases from 46% to less than 10% for H_2O_2 after 80 h. Although no activity increase is obtained with the PDMS embedded catalysts for epoxidation reactions, a clearly important *t*BHP efficiency increase is seen.

3.4. Regeneration

After reaction with the $[Mn(bpy)_2]^{2+}$-NaY-PDMS catalyst at 293 K, *catalyst regeneration* by drying in an oven can have detrimental effects on the catalytic membrane. The chosen regeneration procedure consists of rinsing the PDMS catalyst in a solvent to remove the oxidation products and drying the membrane up to 333 K under vacuum. It can be re-used more than 3 times. In FT-IR shown in Fig. 6, the intensity of asymmetric deformation bands of CH_3 in $SiCH_3$ at 1413 and 1445 cm^{-1} and the C–N and C–C stretches at 1442, 1475 and 1493 cm^{-1} remain comparable. The pink colour from the MLCT of the complexes was maintained, the intensity of this band in UV-Vis did not decrease significantly. It was not maintained when the membrane was dried in the oven at 393 K, leading to the membrane turning brown.

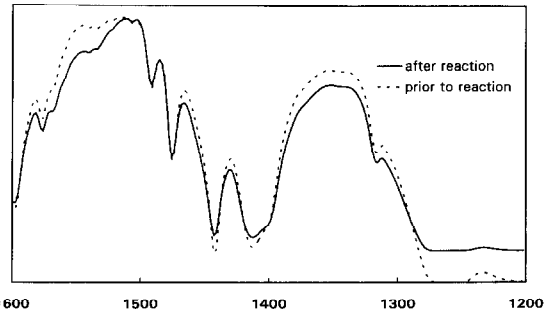

Fig. 6. FT-IR spectra of the c*is*-$[Mn(bpy)_2]^{2+}$-NaY-PDMS membrane prior to and after a reaction with *t*BHP.

4. Conclusions

A new system for olefin epoxidation catalysis with *t*BHP and *cis*-$[Mn(bpy)_2]^{2+}$-NaY-PDMS is presented. The sorption of solvents, substrates and oxidantia in the composite catalyst system $[Mn(bpy)_2]^{2+}$-NaY-PDMS plays a crucial role in the realisation of a catalytic system with good epoxidation yields and high peroxide efficiency. The PDMS embedded catalyst system shows analogous catalytic activity to $[Mn(bpy)_2]^{2+}$-NaY with *t*BHP and reduced activity with H_2O_2. In the PDMS embedded catalyst system the solvent primarily affects membrane accessibility. For styrene and cyclohexene epoxidation with *t*BHP, the activity increases in the solvent sequence acetone, octane, olefine. Brönsted acid sites in $[Mn(bpy)_2]^{2+}$-NaY-PDMS create bifunctionality and explain the high amount of opening of the oxirane ring after epoxidation. An increase in catalyst life-time results from the PDMS that forms an oxidant concentration barrier. The PDMS membrane also leads to higher *t*BHP efficiency in olefin epoxidation, in combination with the easier catalyst handling this may form an incentive to use such composite catalysts. Threefold regeneration is achieved by rinsing the PDMS catalyst in a solvent to remove the oxidation products and drying the membrane up to 333 K under vacuum, oberving minimal activity loss.

Acknowledgements

The authors acknowledge IUAP-PAI sponsering from the Belgian Federal Government. PPKG and IFJV are grateful to the Belgian National Fund for Scientific Research (NFWO) for a grant as doctoral and post-doctoral researcher, respectively.

References

[1] I. Fridovich, Annu. Rev. Biochem., 44 (1975) 147–159.
[2] G.D. Lawrence and D.T. Sawyer, Coord. Chem. Rev., 27 (1978) 173–193.

[3] G.W. Brudvig and R.H. Crabtree, Prog. Inorg. Chem., 37 (1991) 99–142.
[4] C.C. Addison and M. Kilner, J. Chem. Soc. A (1966) 1249.
[5] S.R. Cooper and M. Calvin, J. Am. Chem. Soc., 99 (1977) 6623.
[6] R.F. Parton, I.F.J. Vankelecom, M. Casselman, C. Bezoukhanova, J.B. Uytterhoeven and P.A. Jacobs, Nature, 370 (1994) 541.
[7] D. De Vos, P.P. Knops-Gerrits, R. Parton, B. Weckhuysen, P.A. Jacobs and R.A. Schoonheydt, J. Incl. Phen. Mol. Recogn. Chem., 21 (1995) 185.
[8] D. De Vos, F. Thibault-Starzyk, P.P. Knops-Gerrits, R.F. Parton and P.A. Jacobs, Macromol. Symp., 80 (1994) 157.
[9] K. Maruszewski, D. Strommen, K. Handrich and J. Kincaid, Inorg. Chem. 30 (1991) 4579–4582.
[10] P.P. Knops-Gerrits, D. De Vos, F. Thibault-Starzyk and P.A. Jacobs, Nature, 369 (1994) 543.
[11] P.P. Knops-Gerrits, F. Thibault-Starzyk, P.A. Jacobs, Stud. Surf. Sci. Catal., 84B (1994) 1411–1418
[12] P.P. Knops-Gerrits, C.A. Trujillo, B.Z. Zhan, X.Y. Li, P. Rouxhet, P.A. Jacobs, Topics in Catal., 3 (1996) 437–449.
[13] D.E. Vos, P.L. Buskens, D.L. Vanopper, P.P. Knops-Gerrits, P.A. Jacobs, in J.M. Lehn et al. (Editors), Comprehensive supramolecular chemistry, Pergamon, Oxford, 1996, Vol. 7, Ch. 22, pp. 647–669.
[14] T. Bein, in J.M. Lehn et al. (Editors), Comprehensive supramolecular chemistry, Pergamon, Oxford, 1996, Vol. 7, Ch. 22, pp. 579–619.
[15] I. Rubinstein and A. Bard, J. Am. Chem. Soc., 102 (1980) 6641.
[16] J.M. Calvert and T.J. Meyer, Inorg. Chem., 20 (1981) 27 and 21 (1982) 3978.
[17] H.C. Tung, C. Kang and D.T. Sawyer, J. Am. Chem. Soc., 114 (1992) 3445.
[18] B.A. Moyer, M.S. Thompson and T.J. Meyer, J. Am. Chem. Soc. 102 (1980) 2310–2312.
[19] J.C. Dobson, W.K. Seok and T.J. Meyer, Inorg. Chem., 25 (1986) 1514–1516.
[20] P.P. Knops-Gerrits, M.L. Abbé, W.H. Leung, A.M. Van Bavel, G. Langouche, I. Bruynseraede, P.A. Jacobs, Stud. Surf. Sci. Catal., 101 (1996) 811–820.
[21] R.A. Leising and K.J. Takeushi, Inorg. Chem., 26 (1987) 4391–4393.
[22] W.R. McWhinney and J.D. Miller, Adv. Inorg. Chem. Radiochem., 12 (1967) 135–215.
[23] E.D. McKenzie, Coord. Chem. Rev., 6 (1971) 187–216.